^{166}Er Mössbauer study of magnetic ordering in Er_3Ge_4

D.H. Ryan[1], J.M. Cadogan[2] and R. Gagnon[1]

[1]*Physics Department and Centre for the Physics of Materials, McGill University, 3600 University Street, Montreal, Quebec H3A 2T8, Canada*

[2]*School of Physics, The University of New South Wales, Sydney, Australia*

^{166}Er Mössbauer spectroscopy has been used to study the magnetic ordering of erbium moments in Er_3Ge_4. We find that the average Er moment is less than 80% of its free-ion value, and we have confirmed that at 1.5 K, the moment associated with Er atoms on the $4c$ site is 15% smaller than that on the $8f$ site. The hyperfine field at the $4c$ site declines much more rapidly with increasing temperature than that at the $8f$ site, however our data show no indication of the spin re-orientation claimed to occur at ~4 K.

75.50.-y 75.50.Ee 76.80.+y

I. INTRODUCTION

X-ray[1] and neutron[2] diffraction studies of Er_3Ge_4 have shown that it adopts an orthorhombic structure (Cmcm, space group #63) with two Er sites ($Er_1(8f)$, $Er_2(4c)$) and three Ge sites. Analysis of neutron diffraction data below the Néel temperature (T_N) of 7.3 K revealed a two-dimensional canted antiferromagnetic triangular structure with very different moments associated with the two crystallographically distinct Er sites. At 1.5 K these were reported to be 7.32(5) μ_B/Er at the $Er_1(8f)$ site, and 6.37(6) μ_B/Er at the $Er_2(4c)$ site[2]. In addition, distinct temperature dependences were found for the two Er sites, with the Er–$4c$ moment falling much more rapidly than the Er–$8f$ moment. Finally, a weak ($\sim 1°$) spin reorientation was claimed to occur at the $8f$ site around 4 K associated with a slight change in the temperature dependence of the Er-$4c$ moment.

Two calorimetric studies of Er_3Ge_4 have been made[3,4]. Janssen *et al.*[3] reported a sharp peak at 6.9 K, corresponding to T_N and a weak shoulder around 4 K which they associated with the spin reorientation seen by neutron scattering. They commented that their integrated magnetic entropy is rather low, but their heat capacity for Er_3Ge_4 lies far below that reported by the same group for the non-magnetic analogue Lu_3Ge_4[5]. By contrast, a more recent calorimetric study[4] revealed two clear features in the low-temperature heat capacity. The upper one (~7 K) is clearly associated with the onset of antiferromagnetic order, while a second peak at ~3.5 K was linked to the spin reorientation at 4 K reported in the neutron diffraction study[2]. While the total entropy change below T_N appears quite reasonable, the entropy associated with the 3.5 K peak is remarkably large, accounting for about a third of the total entropy change observed between 0 K and T_N (7.3 K). The size of the peak at ~3.5 K suggests either the presence of a magnetic impurity (which would bring it more into line with the earlier work[3]), or that far more than just a 1° spin reorientation occurs at 3.5 K in Er_3Ge_4.

Given the inconsistencies between the two calorimetric studies, and the mis-match between the thermal and neutron diffraction signatures of the event at 3.5 K, we felt that a more local and direct study of the intrinsic magnetic ordering behaviour was needed. We report here the results of a ^{166}Er Mössbauer investigation of Er_3Ge_4. The Er moments on the two sites are significantly reduced from the free-ion $9\mu_B$/Er, in full agreement with the neutron diffraction data[2]. We clearly resolve the moment difference between the two Er sites, and confirm their very different temperature dependences. However, neither our bulk characterisation nor our microscopic measurements yield any significant indication of the magnetic changes claimed to occur below T_N.

II. EXPERIMENTAL METHODS

Samples were prepared in a tri-arc furnace with a base pressure of better than 6×10^{-7} mbar. Stoichiometric amounts of the pure elements (Er (99.9%) and Ge (99.999%)) were melted several times under pure (less than 1 ppm impurity) argon to ensure homogeneity. The ingot was then annealed under vacuum at 800°C for three weeks and water-quenched.

Powder x-ray diffraction measurements were made at ambient temperature using Cu K_α radiation and analysed using GSAS[6] to extract lattice parameters and check for impurities. Data for the specific sample used in this study are shown in Fig 1. Analysis confirms that this sample is primarily composed of the orthorhombic Er_3Ge_4 phase, with a ~5 wt.% ErGe impurity.

Basic magnetic characterisation was carried out on a Quantum Design Physical Properties Measurement System (PPMS) susceptometer/magnetometer at temperatures from 1.8 K to RT. AC Susceptibility (χ_{ac}) measurements were made with a driving field of 1 mT at 137 Hz. Magnetisation measurements were made in fields of up to 6 Tesla.

Mössbauer measurements were obtained using 1 GBq ^{166}Ho sources prepared by neutron-activation of $Ho_{0.6}Y_{0.4}H_2$ in the SLOWPOKE reactor at Ecole Polytechnique, Montréal. The spectrometer was operated vertically with both source and sample cooled in a helium-flow cryostat and gave a linewidth of 2.5 mm/s (HWHM) for an $ErFe_2$ standard at 4.5 K. Independent temperature control of the source was used to keep it at or above 5 K to avoid relaxation-induced line broadening which we have observed at lower source temperatures. A He/Ne laser interferometer was used to provide simultaneous calibration of all spectra. With the spectrometer operated in sine-mode, at a V_{max} of ∼82 mm/s, the calibration drift in V_{max} was less than 0.02 mm/s. Velocity calibration was cross-checked using $ErFe_2$[7].

The spectra below 2.5 K could be fitted using a conventional non-linear least-squares minimisation routine with line positions and intensities derived from a full solution to the nuclear Hamiltonian for the ^{166}Er 2→0 transition. The hyperfine fields at 1.5 K yielded the moment ratio for the two Er sites, allowed direct comparison with the Er moments deduced from neutron diffraction data and provided confirmation of the field to moment scaling factor. The full Hamiltonian fits were also used to check the static limits of the fitting procedures employed for spectra obtained at higher temperatures where relaxation effects became increasingly important.

Slow electronic relaxation effects are ubiquitous in ^{166}Er Mössbauer spectra, occurring in both oxides[8] and alloys[9]. Er_3Ge_4 is no exception. The relaxation broadening effects observed in the higher temperature spectra were dealt with in two ways. Firstly, the dynamics were included explicitly in the fits by using a stochastic model[10] in which the hyperfine field at an Er site fluctuates randomly between $\pm B_{hf}$ with some average frequency ν. Both $|B_{hf}|$ and ν were taken as independent for the two Er sites. This procedure yields good quality fits that are formally correct, however the derived parameters cannot be used in a direct comparison with the neutron diffraction data. The moments obtained in a neutron scattering experiment represent an instantaneous ensemble average over the Er moments in the system. By contrast, the hyperfine field in a Mössbauer spectrum is a time-average at the probe site that is then averaged over many observations across the whole system. The dynamic fits give information on the relaxation rates, and on the magnitude of the fields (and hence the moment) involved in the dynamic behaviour, but they do not yield the time-averaged Er moments. To obtain this key parameter, we need the average magnetic splitting seen in the spectrum, and we turned therefore to a second, simpler, static model using Gaussian distributions of hyperfine fields. This model yields a direct measure of the average hyperfine fields at the two Er sites, and uses a Gaussian field distribution to generate the line broadening associated with the relaxation effects. As with the dynamic model above, $<B_{hf}>$ and $\sigma_{B_{hf}}$ were treated as independent at the two Er sites. The static fits were as good as the dynamic ones up to about 6 K, above this temperature, dynamic fits were clearly superior.

III. BASIC MAGNETIC CHARACTERISATION

χ_{ac}(T) for Er_3Ge_4 (Fig. 2) exhibits a single clear cusp at T_N=7.2(1) K, in full agreement with previous reports[2–4]. The out of phase signal (χ'') mirrors the χ' cusp with a weaker, more rounded peak, then rises sharply on cooling through 4 K. Fitting the high temperature section (T≥ 40 K) of the χ' data in Fig. 2 to a Curie-Weiss function yields a paramagnetic Curie temperature of $\theta_P = -4.40(2)$ K, consistent with antiferromagnetic ordering. The fit also yields an effective Er moment of 10.5(1) μ_B, somewhat larger than the expected paramagnetic moment of 9.58 μ_B, but consistent with values reported for $ErGe_2$[11] and $ErGe_3$[12].

Magnetisation curves below T_N are clearly 'S'-shaped, with a marked increase starting at ∼1 T (Fig. 3). This form weakens with increasing temperature, but is not lost until T_N. We could find no change in either the position or size of the break in slope that we could associate with the 3.5 K peak in the heat capacity[4], it therefore appears to be a field-driven change in the magnetic structure that is unrelated to any temperature-driven spin reorientation[2]. The magnetisation curves were far from saturation in 6 T, however the maximum response at 2 K corresponds to an average moment of 5.2 μ_B/Er, a remarkably large fraction of the 7.0 μ_B/Er possible according to the neutron diffraction data[2], suggesting than an almost complete rearrangement of the antiferromagnetic spin structure occurs in only a few Tesla. The relative ease with which the zero-field spin arrangement is destroyed reflects the rather weak exchange interactions in this system, and is consistent with the absence of evidence for the 4 K spin reorientation in the high-field data. However, the region below about 1 T was essentially linear at most temperatures, and a fit to data obtained below 0.6 T (so that the measurements at all temperatures were linear) yields the dc susceptibility (χ_{dc}) shown as circles in Fig. 4. χ_{dc} shows behaviour similar to that seen in χ', with a peak at T_N. However, there is an apparent inflection at ∼4 K, which might suggest that there is some change in magnetic behaviour below T_N.

As will be clear from the ^{166}Er Mössbauer work that follows, the weak inflection in χ_{dc}(T) and the upturn in χ''(T) are the *only* indications of the 4 K spin reorientation[2] or the 3.5 K heat capacity feature[3,4] that we have been able to observe in this study. Neither feature constitutes compelling evidence for any change in the intrinsic magnetic behaviour of Er_3Ge_4 below T_N.

IV. ^{166}ER MÖSSBAUER RESULTS

The ^{166}Er Mössbauer spectrum of Er_3Ge_4 at 2.5 K (Fig. 5) shows that the two Er sites are fully resolved, exhibiting quite different magnetic hyperfine fields (B_{hf}), as expected from the earlier neutron diffraction data[2]. Four of the five magnetic lines clearly have two components (the central line results from the 0→0 hyperfine transition and is not affected by a magnetic hyperfine field), Using the simple Gaussian model, we find that the average fitted area of the more widely split pentet between 1.5 K and 6 K is 65.2±2.3% of the total area, fully consistent with the 2:1 ratio expected for Er in the $8f$:$4c$ sites. (Above 6 K the relaxation broadening is too severe for our simple Gaussian distribution to yield a meaningful fit) This clear agreement on the relative areas of the two sub-spectra permits unambiguous assignment of each component to Er atoms in specific crystallographic sites. The two hyperfine fields at 1.5 K are 654(1) T for the $8f$ site and 553(2) T for the $4c$ site, giving a field ratio of 1.183(5):1, which compares extremely well with the moment ratio of 1.15(2):1 determined by neutron diffraction at the same temperature[2]. These fields (and the neutron derived Er moments) are well below the 770 T and 9 μ_B expected for free-ion Er in a pure $\frac{15}{2}$ ground state[13], therefore there must be a substantial crystal-field induced admixture of other states, even at 1.5 K. Reduced Er moments appear to be a common feature of binary Er–Ge alloys[14].

Visual inspection of the two components in the Mössbauer spectra in Fig. 5 reveals that they have very different temperature dependences, with the $8f$ sub-spectrum remaining essentially unchanged, while the $4c$ sub-spectrum collapses and broadens rapidly with increasing temperature. This behaviour is most appropriately fitted using the two-site relaxation model discussed above. The results of such fits, summarised in Fig. 6, clearly show the very different thermal evolution of the moments at the two Er sites. The hyperfine field at the $8f$ site is essentially temperature independent, with relaxation effects setting in only at T_N, however the growth of the relaxation rate at this point is extremely abrupt. By contrast, the field at the $4c$ site declines continuously and relaxation broadening appears above 2.5 K, well below T_N. Above 6.5 K the relaxation effects at the $4c$ site were such that either ν or $|B_{hf}\,|$ had to be constrained to obtain a stable fit, and so values are not plotted in Fig. 6. Relaxation model fits to the spectra obtained between 5 K and 8 K are shown in Fig. 7. While we cannot make a direct comparison between $|B_{hf}\,|$ from the dynamic fits and μ_{Er} from neutron diffraction, we can clearly see that neither $|B_{hf}(T)|$ nor $\nu(T)$ for the Er-$4c$ site show any anomaly around 4 K where the spin reorientation is claimed to occur. Only a linear increase in $\nu(T)$, and a smooth thermal decline of $|B_{hf}(T)|$ is observed. The onset of relaxation at the $4c$ site is observed just above 2.5 K, and while it is tempting to associate this behaviour with the 3.5 K/4 K features observed previously, the temperature mis-match is a little large, and there is no obvious way to link a small change in moment direction ($\sim 1^\circ$) with a marked increase in relaxation rate.

Since the dynamic fits, while formally correct, do not yield estimates for the average Er moments at the two sites that can be compared directly with the results of neutron diffraction measurements, we turn to the static model. Fig. 8 shows the average hyperfine fields at the two sites derived from the static, Gaussian-broadened model, plotted versus temperature. The free-ion hyperfine field for 9 μ_B on Er is 770.5±10.5 T[13]. There will be an additional contribution of ∼14.1±2.1 T from parent conduction electron polarisation[15] in a metallic environment, giving a total field of 784.6±10.7 T and a moment to field conversion factor of 87.2±1.2 T/μ_B. The ratio between our average hyperfine field and the reported average Er moment[2] at 1.5 K is 88.3(5) T/μ_B (where the error comes almost entirely from uncertainties in the neutron diffraction moments), in complete agreement with our estimated conversion factor. Taking the scaling factor as 87.2 T/μ_B allows us to make a direct comparison between our measured hyperfine fields at the two Er sites and the two neutron diffraction derived moments[2] (open symbols in Fig. 8). The absolute agreement at 1.5 K is excellent. As with the dynamic fits shown in Fig. 6, the hyperfine field at the $8f$ site shows very little temperature dependence, dropping slightly above 6.5 K as relaxation effects start to become important at this site. However, even at 8 K the splitting of the $8f$ sub-spectrum is still over 90% of its value at 1.5 K (Fig. 8). By contrast, from 1.5 K to 6.5 K the hyperfine field at the $4c$ site tracks the reported temperature dependence of the Er moment at that site remarkably well, with one important difference: we again see no evidence of the decrease at 4 K deduced from analysis of the neutron diffraction data[2] and attributed to the spin reorientation. The range of temperatures over which we obtain agreement between $\mu_{Er}4c$ and $B_{hf}4c$ clearly indicates that our simple static analysis does indeed yield a meaningful estimate of the average Er moment at this site, even in the presence of significant dynamic broadening. The time-averaged moment derived from Mössbauer spectroscopy matches the ensemble averaged moment deduced from neutron diffraction.

Given the excellent overall agreement and the enhanced precision provided by the ^{166}Er Mössbauer measurements compared with neutron diffraction, the absence of a break in slope in $B_{hf}(T)$ for the $4c$ site is highly significant. Within the uncertainty of our measurements (<0.4%), there is no change in B_{hf} at the $4c$ site beyond the expected smooth thermal evolution. This observation is supported by both the static and dynamic analyses of the spectra, although only the static model provides numbers that can be compared directly with the neutron scattering moments. Our ^{166}Er Mössbauer spectra provide clear confirmation of the reduced Er moments and their distinct temperature dependences, but the spectra show no changes around 4 K that we could associate with a spin reorientation, or any other change in the intrinsic magnetic order.

V. DISCUSSION

It is clear that exchange interactions in this system are relatively weak ($T_N \sim 7$ K, $\theta_P \sim -4.4$ K), and the reduced Er moments point to significant crystal-field quenching ($\sim$27% at the 4c site). In addition, the distinct ordering directions at the two Er sites coupled with the failure of the magnetisation to saturate in 6 T, indicate that magnetocrystalline anisotropy plays a significant role in the magnetic ordering.

In order to develop some insight into the differences in both the moment magnitudes and their dynamics, we turn to the crystal-field environments of the two Er sites. Taking lattice parameters and atomic positions from neutron diffraction[2], and using the BLOKJE program[16] to determine the Wigner-Seitz cells and hence the nearest-neighbour environments, we find that both Er sites are fully coordinated by germanium atoms (Table I). We then used point-charge calculations to determine the crystal-field parameters at the two Er sites. We recognise that this is a severe approximation, especially in a metallic environment, but it should yield a reasonable description of the site symmetries and relative magnitudes of the terms within a given order. Parameters were calculated out to 6^{th} order using orthogonal axes chosen coincident with the crystallographic axes. Values for the 2^{nd} order terms are shown in Table I.

The dominant contribution at the $4c$ site is clearly the diagonal A_{20} term, with the only off-diagonal contribution being down by almost a factor of two. The negative sign for A_{20} taken with the measured easy $c-$axis ordering direction at this site[2] implies that the effective charge on the germanium ions is positive (within this point-charge approximation). By contrast, the sign of A_{20} at the $8f$ site is positive, indicating that the c-axis cannot be the easy axis at this site, however, the environment of the $8f$ site is dominated by off-diagonal terms, particularly A^s_{21}. We can eliminate this off-diagonal term by rotating our coordinate system (in a procedure analogous to identifying the principal axis system for the electric field gradient (*efg*) in a Mössbauer measurement) and thereby determine the easy axis predicted by our point-charge approximation. We obtain a canting angle of 40° away from c in the $bc-$plane, which compares remarkably well with the reported value for this angle of 35.5(3)°[2].

Er^{3+} is a Kramers ion with $J = \frac{15}{2}$ and so in the paramagnetic state the electronic energy levels comprise eight Kramers doublets. Using the results of our point charge calculations to 2^{nd} order, and assuming a standard 50% screening, yields splittings between the ground and first excited states of $\Delta E(4c) = 17.1$ K and $\Delta E(8f) = 47.5$ K. The full energy level diagram for the two sites, without the exchange splitting of $\sim$7 K is shown in Fig. 9. It is clear that the overall splitting of the electronic levels is much greater at the $8f$ site than at the $4c$ site, and it is this larger level splitting that leads to the much slower relaxation of the Er^{3+} moment at the $8f$ site.

The neutron diffraction data provided two signatures of the spin reorientation event at $\sim$4 K[2]: (i) a change of somewhat less than 1° in the ordering direction of the moments on the $8f$ site, and (ii) a marked decrease in the moment on the $4c$ site on heating through $\sim$4 K. Even in an ideal system, ^{166}Er Mössbauer spectroscopy would not be able to resolve so small a change in ordering direction, however it is clear from Fig. 5 that the second signature is well within the resolution of our data. There is no change in B_{hf} at the $4c$ site, beyond the expected smooth thermal evolution. We do not see any break in the temperature dependence. This conclusion is independent of the analysis model used to account for the observed dynamics. Furthermore, the excellent agreement with the behaviour of the moment at the $4c$ site both above and below the 4 K event (Fig. 8), coupled with the break in slope in the neutron diffraction data being close to the reported uncertainties would suggest that interpretation of the diffraction data in terms of a spin reorientation may be equivocal. Such a view would be more consistent with a heat capacity measurement that shows only a weak shoulder around 4 K[3], and not with data exhibiting a large peak[4]. The complexity of the Er–Ge binary phase diagram coupled with the fact that none of the binary phases around Er_3Ge_4 melts congruently[17] makes some level of impurity almost inevitable. Indeed, none of our Er–Ge alloys were completely single-phase, and the sample of Er_3Ge_4 used in this study contained a $\sim$5 wt.% ErGe impurity (see Fig 1). Our preliminary investigation of neighbouring phases in this system[14] has revealed that while ErGe does not lead to any interference, Er_2Ge_3 orders at 4.0±0.1 K. This latter phase is extremely close in composition to Er_3Ge_4 (40 at.% Er *vs.* 43 at.%), and differing levels of Er_2Ge_3 impurities might account for the differences between the two calorimetric studies[3,4], and would not be inconsistent the claimed spin reorientation temperature.

VI. CONCLUSIONS

Er_3Ge_4 orders antiferromagnetically below T_N=7.2(1) K. In the ordered state, the Er atoms located on the two crystallographic Er sites have different moments and those moments exhibit distinct temperature dependences. These results are in complete agreement with previous neutron diffraction work[2]. However, we observe no significant changes in our data below T_N, and so find nothing to suggest the existence of a spin-reorientation transition around 4 K. The ordering directions of the moments at the two Er sites and their distinct temperature dependences can be understood in terms of the crystal field environments of the erbium ions in this structure.

VII. ACKNOWLEDGMENTS

This work was supported by grants from the Natural Sciences and Engineering Research Council of Canada, Fonds pour la formation de chercheurs et l'aide à la recherche, Québec, and the Australian Research Council. The authors are grateful to Dr. G. Kennedy at the Ecole Polytechnique SLOWPOKE reactor facility, Montréal, where the activation of the ^{166}Ho sources used in this study was carried out.

[1] O.Ya. Oleksyn and O.I. Bodak, J. Alloys and Compounds **210** (1994), 19.
[2] P. Schobinger-Papamantellos, O. Oleksyn, C. Ritter, C.H. de Groot and K.H.J. Buschow, J. Magn. Magn. Mater. **169** (1997), 253.
[3] Y. Janssen, E. Brück, F.E. Kayzel, F.R. de Boer, K.H.J. Buschow, O. Oleksyn and P. Schobinger-Papamantellos, J. Magn. Magn. Mater. **177–81** (1998), 1147.
[4] Y.Y. Chen, Y.D. Yao, Y.S. Lin, C.L. Chang, H.H. Hamdeh and J.C. Ho, Phys. Rev. **B61** (2000), 58.
[5] O. Zaharko, P. Schobinger-Papamantellos, W. Sikora, C. Ritter, Y. Janssen, E. Brück, F.R. de Boer and K.H.J. Buschow, J. Phys.: Condens. Matter **10** (1998), 6553.
[6] A.C. Larson and R.B. von Dreele 1985–94, Los Alamos National Laboratory, Report LAUR 86-748, (1994) (unpublished).
[7] J.A. Hodges, G. Jehanno, A. Schuhl and Y. Berthier, Hyp. Int. **11** (1981), 29.
[8] I. Nowik and H.H. Wickman, Phys. Rev. Lett. **17** (1966), 949; M. Eibschütz, R.L. Cohen, K.W. West, Phys. Rev. **178** (1969), 572.
[9] W. Wiedemann and W. Zinn, Phys. Lett. **24A** (1967), 506; P.C.M. Gubbens, A.M. van der Kraan and K.H.J. Buschow, Phys. Rev. **B39** (1989), 12548.
[10] M. Blume and J.A. Tjon, Phys. Rev. **165** (1968), 446.
[11] O. Oleksyn, P. Schobinger-Papamantellos, C. Ritter, C.H. de Groot and K.H.J. Buschow, J. Alloys and Compounds **252** (1997), 53.
[12] P. Schobinger-Papamantellos, G. André, J. Rodríguez-Carvajal, C.H. de Groot and K.H.J. Buschow, J. Alloys and Compounds **232** (1996), 165.
[13] B. Bleaney, in "Handbook on the Physics and Chemistry of Rare Earths", Vol. 11, Chapter 77 (1988) K.A. Gschneidner Jr. and L. Eyring (eds.) Elsevier Science Publishers (Amsterdam).
[14] D.H. Ryan, J.M. Cadogan and R. Gagnon (unpublished results).
[15] Y. Li, C. Carboni, J.W. Ross, M.A.H. McCausland and D.St.P. Bunbury, J. Phys.: Condens. Matter **8** (1996), 865.
[16] L. Gelato, J. Appl. Cryst. **14** (1982), 151.
[17] "Binary alloy phase diagrams" T.B. Massalski, J.L. Murray L.H. Bennett and H. Baker (eds.) (1986) American Society for Metals (Metals Park, Ohio).

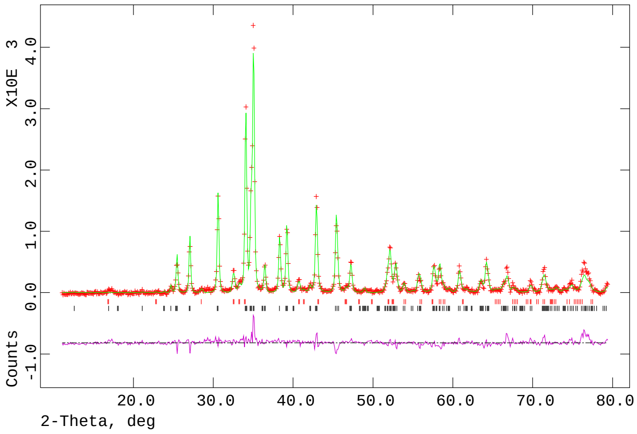

FIG. 1. Cu-K$_\alpha$ x-ray diffraction pattern for Er_3Ge_4 with fit showing Er_3Ge_4 primary phase (lower markers) and ∼5 wt.% ErGe impurity (upper markers).

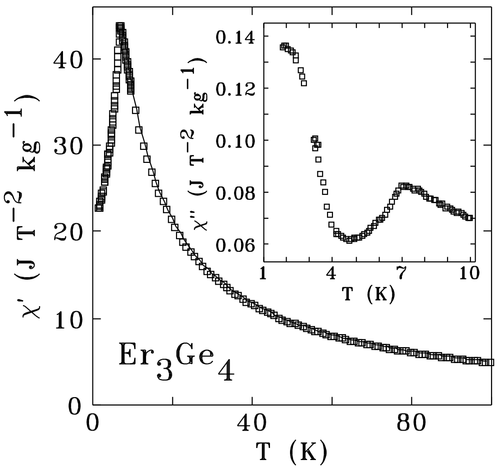

FIG. 2. Temperature dependence of the ac-susceptibility (χ') for Er_3Ge_4 showing the cusp at T_N=7.2(1) K. The solid line is a Curie-Weiss fit discussed in the text. Inset shows the out of phase (loss) response (χ'') which exhibits a peak at T_N, and then rises sharply below 4 K.

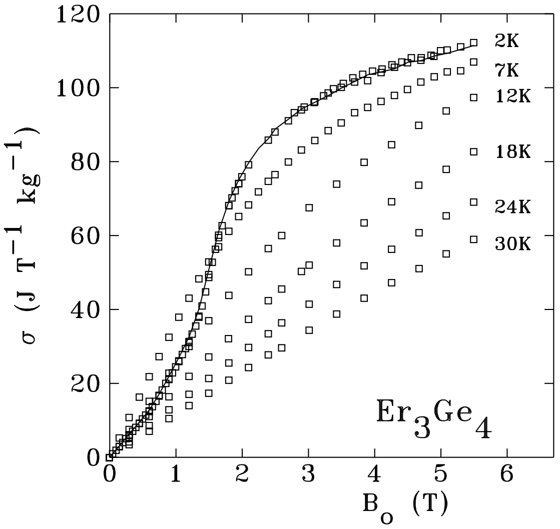

FIG. 3. Magnetisation curves for Er_3Ge_4 at various temperatures. The 2 K curve has been highlighted with a solid line to make the S-shape more obvious.

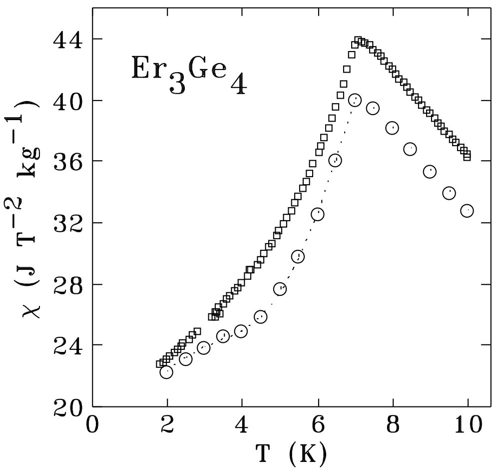

FIG. 4. Comparison of low-field ac-susceptibility (χ') (squares) with the dc-susceptibility (χ_{dc}) obtained below 0.6 T (circles) showing an inflection in χ_{dc}(T) at ∼4 K. The dotted line is a guide to the eye.

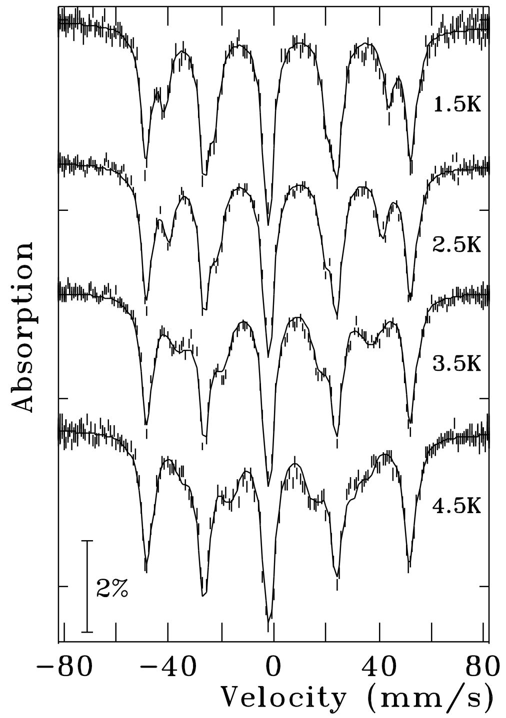

FIG. 5. ^{166}Er Mössbauer spectra of Er_3Ge_4 taken at temperatures well below T_N. The magnetic pentets from the two Er sites are clearly resolved, especially at 2.5 K. The very different temperature dependences of the splittings at the two sites are readily apparent. Solid lines are fits using the Gaussian distribution model described in the text.

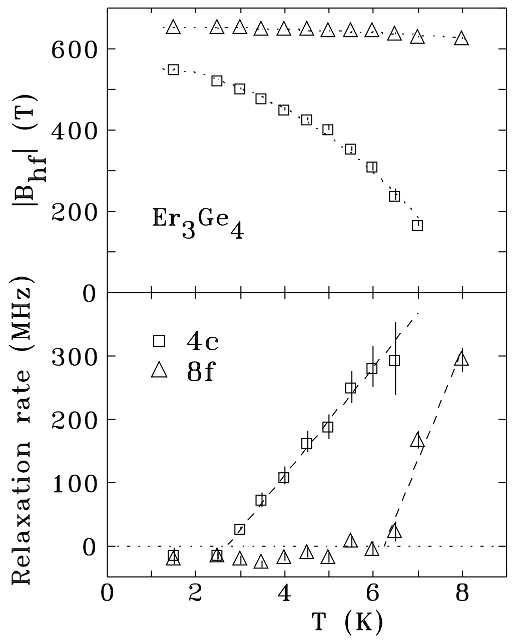

FIG. 6. Parameters derived from the two-site stochastic relaxation model: (Top) $|B_{hf}|$ and (Bottom) relaxation rates at the two Er sites in Er_3Ge_4. The Er-4c site shows a rapid increase in relaxation rate above 2.5 K while the Er-8f site appears static up to T_N. The dashed lines are guides to the eye.

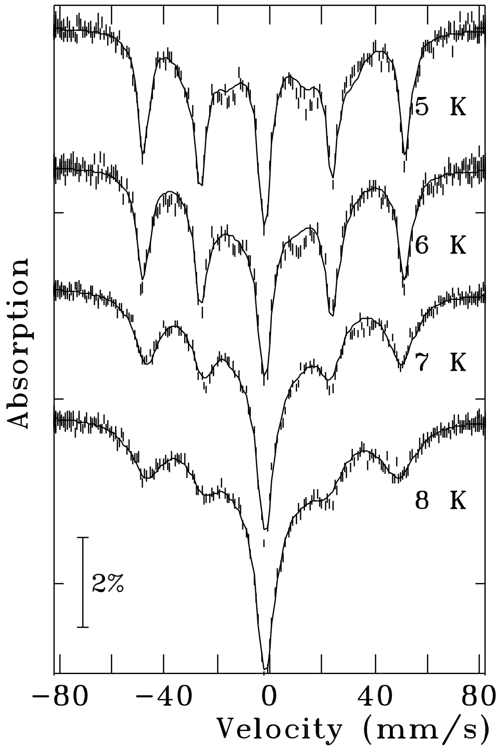

FIG. 7. [166]Er Mössbauer spectra of Er_3Ge_4 taken at temperatures around T_N. The inner pentet due to the Er-4c site is already severely broadened, while the outer pentet associated with the Er-8f site starts to broaden only above 6 K. The solid lines are fits using the two-site relaxation model described in the text.

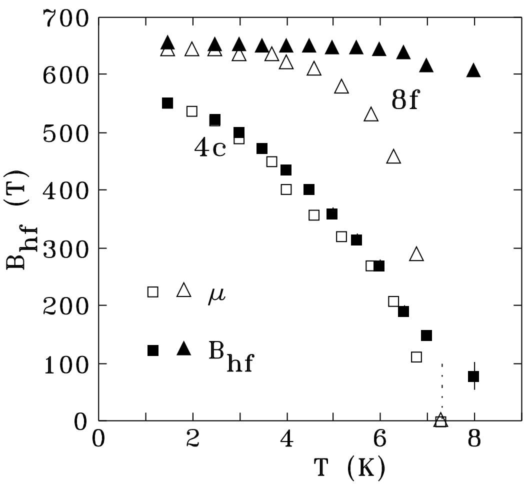

FIG. 8. Temperature dependence of the average [166]Er hyperfine fields at the two Er sites in Er_3Ge_4 (solid symbols) derived from the Gaussian distribution model described in the text. For comparison, the Er moments derived from neutron diffraction data (Ref. 2) are shown as open symbols, scaled by a factor of 87.2 T/μ_B (see text). Errors for the Mössbauer data lie well within the plotted points. The dotted line at 7.2 K marks T_N.

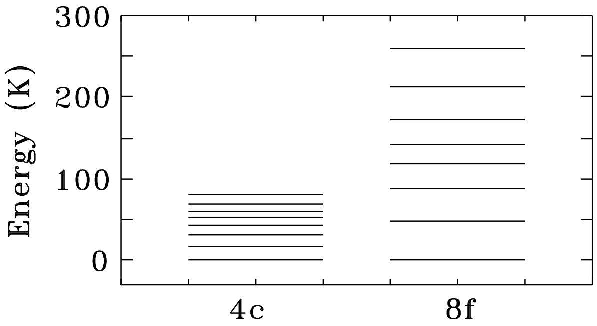

FIG. 9. Er^{3+} energy levels in Er_3Ge_4 for the 4c and 8f sites in Er_3Ge_4.

TABLE I. Point symmetries and local environments for the two crystallographically distinct Er sites in Er_3Ge_4. Also shown are the crystal-field lattice sums to second order. To convert from A_{2m} (in units of K a_0^{-2}, where a_0 is the Bohr radius) to the standard crystal-field parameters B_{2m}, multiply by $1.81\times10^{-3} \times Q_{Ge}$, where Q_{Ge} is the effective point-charge on the neighbouring germanium ions.

Er Site	Er_1 (8f)	Er_2 (4c)
Point symmetry	m..	m2m
1^{st} neighbours	8 Ge	7 Ge
Distances (Å)	2.96–3.04	2.83–3.14
Crystal Field Terms		
A_{20}	+246	−462
A_{21}^c	0	0
A_{21}^s	+5309	0
A_{22}^c	+230	−284
A_{22}^s	0	0